



Cytokine signaling through *Drosophila* Mthl10 ties lifespan to environmental stress

Eui Jae Sung^a, Masasuke Ryuda^b, Hitoshi Matsumoto^c, Outa Uryu^c, Masanori Ochiai^d, Molly E. Cook^e, Na Young Yi^f, Huanchen Wang^a, James W. Putney^g, Gary S. Bird^g, Stephen B. Shears^{a,1}, and Yoichi Hayakawa^{c,1}

^aInositol Signaling Group, Signal Transduction Laboratory, National Institute of Environmental Health Sciences, National Institutes of Health, Research Triangle Park, NC 27709; ^bThe Analytical Research Center for Experimental Sciences, Saga University, Saga 840-8502, Japan; ^cDepartment of Applied Biological Sciences, Saga University, Saga 840-8502, Japan; ^dRadioisotope Division, Institute of Low Temperature Science, Hokkaido University, Sapporo 060-0819, Japan; ^eProtein Expression Core Laboratory, National Institute of Environmental Health Sciences, National Institutes of Health, Research Triangle Park, NC 27709; ^fBiomanufacturing Research Institute and Technology Enterprise, ^gBiomanufacturing Research Institute and Technology Enterprise, North Carolina Central University, Durham, NC 27707; and ¹Calcium Signaling Section, Signal Transduction Laboratory, National Institute of Environmental Health Sciences, National Institutes of Health, Research Triangle Park, NC 27709

Edited by Solomon H. Snyder, Johns Hopkins University School of Medicine, Baltimore, MD, and approved November 13, 2017 (received for review July 12, 2017)

A systems-level understanding of cytokine-mediated, intertissue signaling is one of the keys to developing fundamental insight into the links between aging and inflammation. Here, we employed *Drosophila*, a routine model for analysis of cytokine signaling pathways in higher animals, to identify a receptor for the growth-blocking peptide (GBP) cytokine. Having previously established that the phospholipase C/Ca²⁺ signaling pathway mediates innate immune responses to GBP, we conducted a dsRNA library screen for genes that modulate Ca²⁺ mobilization in *Drosophila* S3 cells. A hitherto orphan G protein coupled receptor, Methuselah-like receptor-10 (Mthl10), was a significant hit. Secondary screening confirmed specific binding of fluorophore-tagged GBP to both S3 cells and recombinant Mthl10-ectodomain. We discovered that the metabolic, immunological, and stress-protecting roles of GBP all interconnect through Mthl10. This was established by *Mthl10* knockdown in three fly model systems: in hemocyte-like *Drosophila* S2 cells, *Mthl10* knockdown decreases GBP-mediated innate immune responses; in larvae, *Mthl10* knockdown decreases expression of antimicrobial peptides in response to low temperature; in adult flies, *Mthl10* knockdown increases mortality rate following infection with *Micrococcus luteus* and reduces GBP-mediated secretion of insulin-like peptides. We further report that organismal fitness pays a price for the utilization of Mthl10 to integrate all of these various homeostatic attributes of GBP: We found that elevated *GBP* expression reduces lifespan. Conversely, *Mthl10* knockdown extended lifespan. We describe how our data offer opportunities for further molecular interrogation of yin and yang between homeostasis and longevity.

stress | longevity | receptor

The field of geroscience takes an interdisciplinary, systems-level approach to the study of aging, by integrating the diverse cellular and organismal stress–response pathways that are activated by intrinsic and extrinsic challenges (1). Pivotal to this approach is the characterization of intertissue signaling cascades that induce adaptive and chronic inflammation (1). Such pathways tend to be highly conserved, and so invertebrates have proved to be productive models for pursuing a molecular understanding of links between inflammation and aging in humans (1, 2). Of special interest to the current study is one particular family of cytokines that are distributed through several insect orders (3, 4); while these peptides are multifunctional, the family is commonly designated by the activity of the founding member: growth-blocking peptide (GBP) (5). This eponymous cytokine was identified from its growth-inhibiting effects in the larval stage of the armyworm, *Pseudaletia separata*, upon parasitization by the wasp *Cotesia kariyai* (5). In *Drosophila* there is a 24-residue, biologically active GBP cytokine that is produced by serine protease cleavage of the C terminus of a larger, precursor protein (3) (Fig. S1). Interestingly, *Drosophila* GBP shares some

sequence similarity with human BD2 (Fig. S1), a member of the immunomodulatory β -defensin family (6).

Biological functions of GBP in *Drosophila* include protection against certain environmental stresses (3), regulation of humoral and cellular innate immune responses (7), and release of insulin-like peptides (ILPs) from the brain in response to nutrient intake (8). However, there has not previously been a molecular rationalization of this cytokine's multiple homeostatic properties. We hypothesized that identification of a GBP cell-surface receptor could provide a molecular basis for understanding the molecular pathways that GBP regulates, and explain the nature by which the various biological activities of this cytokine might be interrelated. We further posited that genetic manipulation of a GBP receptor might provide a basis for systems-level insight into general relationships between inflammation and aging.

Results and Discussion

Identification of a GBP Receptor by High-Throughput Screening of Ca²⁺ Mobilization. We have previously shown that *Drosophila* GBP recruits the PLC/Ca²⁺ signaling pathway to mediate innate immune responses (7, 9). Thus, we conducted a dsRNA library screen for a GBP receptor, using Ca²⁺ mobilization in *Drosophila* S3 cells as a biological readout. This screening was facilitated by our creating a *Drosophila* S3 cell line that hosts a genetically encoded Ca²⁺ sensor, GCaMP3. These cells (S3^{GCaMP3}) were

Significance

Invertebrates are productive models for understanding basic molecular principles that link cytokine-mediated inflammatory pathways to aging in humans. Here, we use a high-throughput dsRNA screen to determine that the multifunctional *Drosophila* cytokine, GBP, is a ligand for the hitherto orphan GPCR, Mthl10. Through genetic manipulation of the GBP/Mthl10 axis in larvae and adult flies, we are able to demonstrate how organismal longevity is interconnected to immunological, metabolic, and stress-protective responses. Our results provide a molecular basis for hypothesizing that a successful defense against environmental insults—be they pathogenic inflammation or non-infective challenges—will ultimately reduce lifespan.

Author contributions: E.J.S., H.W., J.W.P., G.S.B., S.B.S., and Y.H. designed research; E.J.S., M.R., H.M., O.U., M.O., N.Y.Y., H.W., S.B.S., and Y.H. performed research; M.E.C. contributed new reagents/analytic tools; E.J.S., M.R., H.M., O.U., M.O., N.Y.Y., H.W., G.S.B., S.B.S., and Y.H. analyzed data; and E.J.S., M.E.C., S.B.S., and Y.H. wrote the paper.

The authors declare no conflict of interest.

This article is a PNAS Direct Submission.

Published under the PNAS license.

¹To whom correspondence may be addressed. Email: shears@niehs.nih.gov or hayakawa@cc.saga-u.ac.jp.

This article contains supporting information online at www.pnas.org/lookup/suppl/doi:10.1073/pnas.1712453115/-DCSupplemental.

used to record GBP-stimulated Ca^{2+} mobilization (7) during screening of a dsRNA library that targets 1,729 genes encoding transmembrane proteins (Fig. 1 *A* and *B* and Figs. *S2* and *S3* and Dataset *S1*). Each individual dsRNA was screened in replicate plates, generally with good reproducibility (Fig. 1*A*). We adopted a lenient disambiguation approach: A mean Z score of <-1.5 for any dsRNA pair was considered a hit (Dataset *S1*). This minimized false negatives, albeit by generating some false positives (see below). The top 17 hits included several genes that encode known Ca^{2+} -signaling proteins (*Ipr*, *Ca-P60A*, *PMCA*, *Stim*, *Orai*; Fig. 1*B* and Fig. *S2B*) (10, 11), plus four genes encoding cell-surface proteins: *SR-CIV* (scavenger receptor protein); *Pvr* (PDGF/VEGF receptor tyrosine kinase); *Oamb* (octopamine Ca^{2+} signaling/cAMP receptor), and *Mthl10*, an orphan GPCR (12). The *Mthl10* hit was particularly striking: A high Z score mean of -4.6 was obtained from three separate dsRNA pairs (Fig. 1*B* and Dataset *S1*).

We performed secondary screening using independent dsRNAs. The treatment of $S3^{GCaMP3}$ cells with *Mthl10* dsRNA diminished GBP-mediated Ca^{2+} mobilization by 85% (Fig. 1*C–E*). We conducted further experiments with thapsigargin (TG), which, by inhibition of Ca-P60A, exposes Ca^{2+} leak from the endoplasmic reticulum, thereby promoting *Mthl10*-independent, *Orai*-mediated Ca^{2+} entry into the cell (ref. 10 and Fig. *S2B*). The results that we obtained (Fig. 1*C–E* and Fig. *S4*) show that *Mthl10* dsRNA does not indirectly perturb any aspect of Ca^{2+} signaling that bypasses the cell-surface GBP receptor.

Mthl10 is one of 12 members of the *Drosophila* “*Mth* superclade,” which includes *Methuselah* (*Mth*) itself, and 11 *Mth*-like (*Mthl*) paralogs, indicative of the possibility of functional redundancy (12, 13). Within this family, ligand-specific functional significance has previously only been ascribed to *Mth*, which regulates secretion of ILPs in response to the ligand Stunted

(14). Nevertheless, in our primary screen, *Mthl10* was the only hit from within the *Mth* superclade (Dataset *S1*). We also performed follow-up experiments, in which independent dsRNA constructs were used to knock down each member of the *Mth* superclade in $S3^{GCaMP3}$ cells (Fig. *S5*). Only *Mthl10* knockdown attenuated GBP-mediated PLC/ Ca^{2+} signaling (Fig. *S5*). Outside of the *Mth* superclade, there are four more distantly related paralogs, *Mthl1*, 5, 14, and 15, which are not viable GBP receptors as they appear not to encode a ligand-binding ectodomain (12). One of these, *Mthl5*, has been reported to contribute to the development of *Drosophila* heart tube morphology (15). Nevertheless, knockdown of each of these four paralogs did not inhibit GBP-mediated PLC/ Ca^{2+} signaling (Fig. *S5*).

In additional secondary screening, knockdown of either *SR-CIV* or *Oamb* did not inhibit Ca^{2+} mobilization (Fig. 1*E* and Fig. *S6A–C*), indicating these genes are false positives in the primary screen (obtained from only one dsRNA pair; Fig. 1*B*); as stated above, our methodology was expected to yield some false positives. As for loss of Ca^{2+} signaling following *Pvr* knockdown in the primary screen (Fig. 1*B*), that was partly attributed to an “off-target” reduction in cell proliferation (Fig. *S5B*; see also ref. 16). Additionally, loss of *GCaMP3* expression following *Pvr* knockdown ablated GBP-independent fluorescence responses (Fig. *S6D*). Secondary screening using Fluo-4 fluorescence (9) showed that equivalent numbers of control and *Pvr* dsRNA-targeted cells yielded similar GBP-mediated Ca^{2+} responses (Fig. *S6E* and *F*).

Validation of GBP-Binding to *Mthl10*. We used orthologous methodology to interrogate the validity of *Mthl10* as a hit from our primary screen. $S3^{GCaMP3}$ cells were incubated with GBP that was C-terminally tagged with tetramethylrhodamine (TMR; Fig. 2*A* and Fig. *S1*). GBP-TMR retained the ability to mobilize Ca^{2+} ,

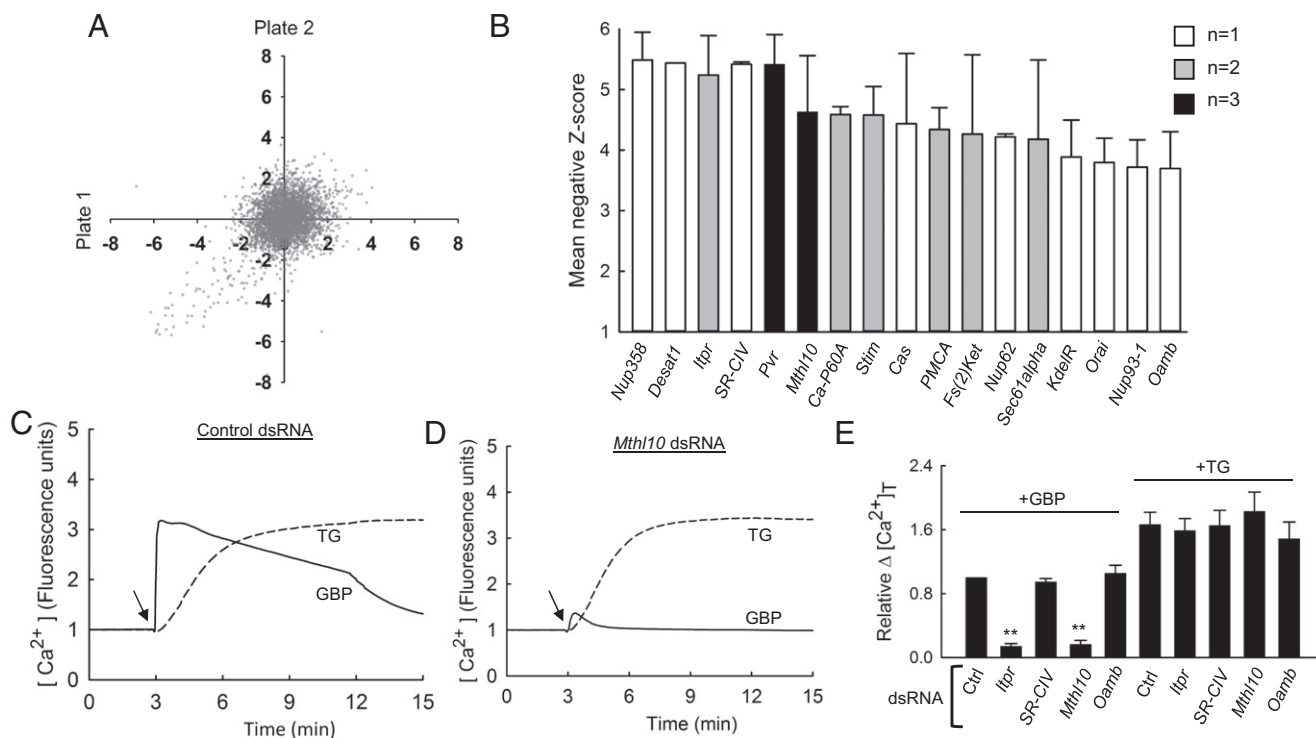


Fig. 1. Application of a dsRNA library to determine that *Mthl10* mediates GBP-dependent Ca^{2+} mobilization in *Drosophila* $S3$ cells. (*A*) Correlation of Z scores from all technical replicates that describe GBP-mediated Ca^{2+} signaling in $S3^{GCaMP3}$ cells in the dsRNA library screen. (*B*) Bar graph depicting the 17 highest Z scores for the indicated genes; the data (mean \pm SD) were obtained from the numbers of dsRNA pairs indicated by the key: white, 1; gray, 2; black, 3. (*C* and *D*) Secondary screening of Ca^{2+} -signaling dynamics in $S3^{GCaMP3}$ cells pretreated with control- or *Mthl10*-dsRNA; arrows show time of addition of either 50 nM GBP or 2 μ M TG. (*E*) Secondary screening of Ca^{2+} responses to GBP or TG in $S3^{GCaMP3}$ cells pretreated with either control dsRNA or dsRNA against the indicated genes. All dsRNAs were $>80\%$ effective except that for *Oamb* (60%; qRT-PCR). Bar graphs show total Ca^{2+} release (i.e., $[Ca^{2+}]_T$) relative to controls (set to unity), calculated by integrating the areas under the Ca^{2+} -mobilization curves (means \pm SEM; $n = 3-4$). $**P < 0.01$.

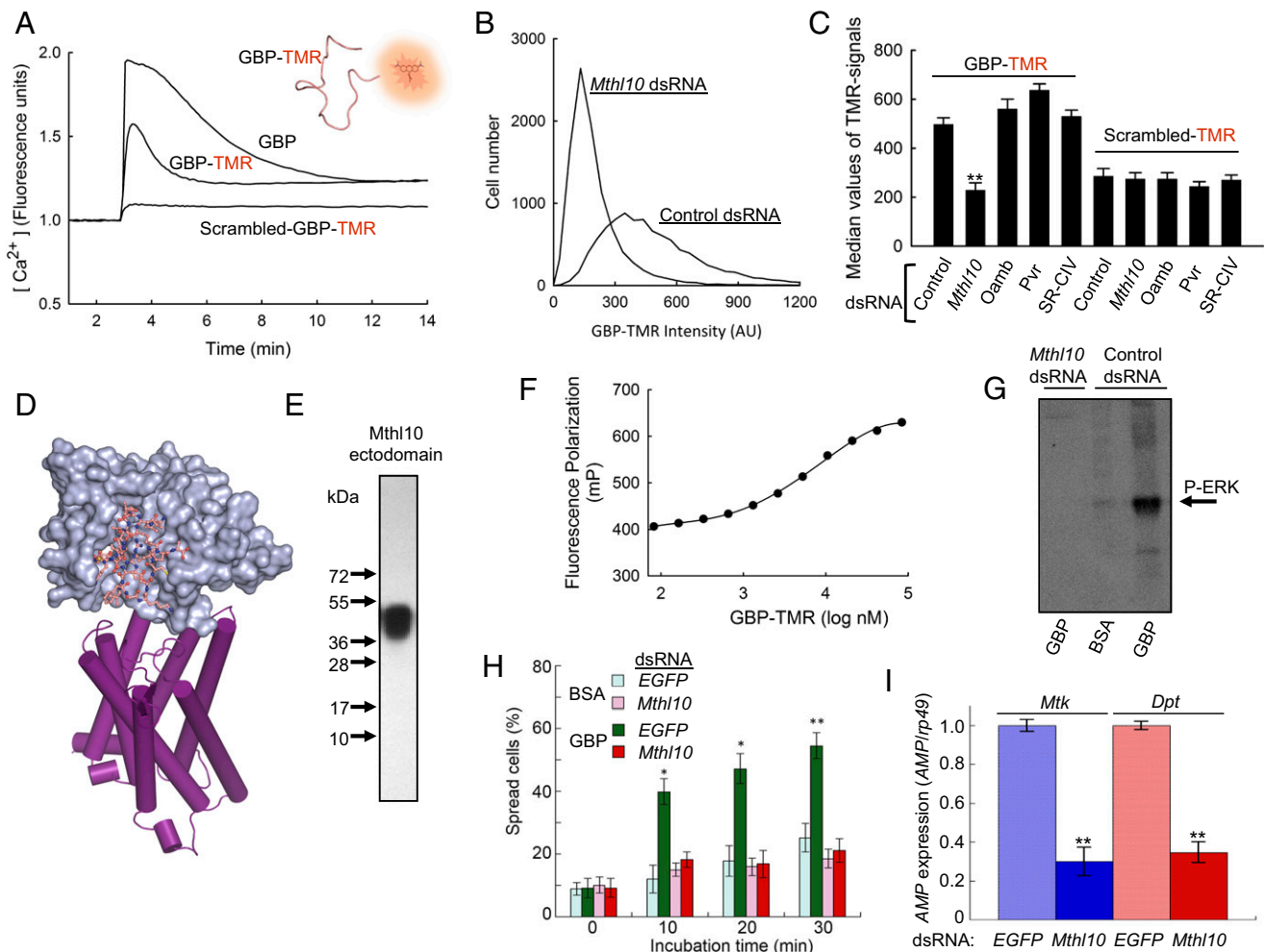


Fig. 2. Mthl10 is a cell-surface receptor for GBP. (A) Representative Ca^{2+} -signaling dynamics in $S3^{GCaMP3}$ cells upon addition of 200 nM of either GBP, GBP-TMR, or "scrambled-GBP"-TMR. (B) Representative analysis by flow cytometry of GBP-TMR association with S3 cells pretreated with either control- or *Mthl10*-dsRNA. (C) Analysis of the association of either GBP-TMR or scrambled-GBP-TMR with S3 cells pretreated with the indicated dsRNA (data are means \pm SEM; $n = 3$). (D) Homology model of the extracellular domain of Mthl10 based on Mth (PDB ID code 1FJR), into which is docked GBP (which is also presented in ribbon format in the A Inset). The ribbon structure for the transmembrane domain comes from homology modeling of the β -2 adrenergic receptor (PDB ID code 3SN6). (E) SDS/PAGE of purified recombinant Mthl10 ectodomain. (F) Representative analysis by fluorescence polarization of GBP-TMR binding to the recombinant extracellular domain of Mthl10. (G) Representative Western assay of ERK phosphorylation ("P-ERK"), detected using anti-phospho-ERK1/2 antibody, following treatment of *Drosophila* S2 cells with either 50 nM GBP or BSA (control) for 3 min. (H) *Drosophila* S2 cells were pretreated with either *Mthl10* dsRNA or control (EGFP) dsRNA, then 50 nM GBP or BSA control was added for the indicated times, and cell spreading was assayed (data are means \pm SEM; $n = 8$). (I) Control- and *Mthl10*-dsRNA treated S2 cells were incubated with 50 nM GBP for 60 min and AMP expression was determined (data are means \pm SEM, $n = 7$). As indicated, * $P < 0.05$, ** $P < 0.01$, versus corresponding control.

albeit with reduced potency (Fig. 2A). Analysis by flow cytometry showed that dsRNA-mediated *Mthl10* knockdown reduced the intensity of the cell-associated fluorophore signal to the level at which a scrambled-GBP-TMR construct (Fig. S1) nonspecifically bound to S3 cells (Fig. 2B and C). These data are consistent with Mthl10 being a GBP receptor. Significantly, knockdown of either *Pvr*, *SR-CIV*, or *Oamb* did not affect specific binding of GBP-TMR to S3 cells, consistent with our conclusion that these genes are false positives in the primary screen (Fig. 2C).

Since *Drosophila* Mthl10 and Mth are paralogs (12, 13), we used the crystal structure of Mth (17) as a template to model the Mthl10 ectodomain; the Mthl10 surface is predicted to have a shallow groove, into which we docked GBP (Fig. 2D). This model aided our design of a gene construct for expression of recombinant, epitope-tagged Mthl10 ectodomain, which we purified to apparent homogeneity; the single smeared band around 45 kDa is indicative of glycosylation (Fig. 2E). Specific binding of GBP-TMR to Mthl10 was confirmed by fluorescence polarization (Fig. 2F). The affinity of binding was estimated to be $6 \pm 0.07 \mu M$

($n = 3$; Fig. 2F), the value likely reflecting a reduction in true GBP affinity due to the addition of the TMR tag (Fig. 2A).

Mthl10 Integrates Immunological and Metabolic Functions of GBP. In *Drosophila* embryos, larvae, and adults, *Mthl10* is expressed in a variety of tissues, including the CNS and the fat body (ref. 13 and Fig. S7A). As a consequence, multiple biological activities of the Mthl10/GBP axis can be anticipated. To assign a specific physiological function for Mthl10 within a single cell type, we knocked down the expression of this receptor in the S2 cell line, a hemocyte-like model (18). In this cell type, GBP regulates both cellular and humoral innate immune activities (7). A key cellular immune response in S2 cells, ERK-dependent cell spreading, was severely attenuated by *Mthl10* knockdown (Fig. 2G and H). Additionally, the GBP-mediated humoral response, i.e., the expression of genes that encode antimicrobial proteins (AMP) such as *Metchnikowin* (*Mtk*) and *Diptericin* (*Dpt*), was also strongly blocked by *Mthl10* knockdown (Fig. 2I).

Adult flies exhibit increased expression of *Mtk* and *Dpt* in response to *GBP* overexpression (4). We found that this immunological response is ablated by knockdown of *Mthl10* in *Drosophila* adults (Fig. 3A). These observations suggested to us that loss of *Mthl10* might increase susceptibility to infection. Indeed, *Mthl10* knockdown dramatically increases mortality rates following infection with the pathogenic bacterium, *Micrococcus luteus* (Fig. 3B).

We found that many other members of the *Mth* superclade are expressed in the brain and eviscerated abdomen of *Drosophila* adults (Fig. S7B). However, none of these paralogs showed off-target changes in their degree of expression following *Mthl10* knockdown (Fig. S7B).

GBP has also been shown to promote AMP production in response to noninfectious stress such as low temperature (4). We exposed *Drosophila* larvae to 4 °C for 16 h, which normally

elevates *Mtk* expression; this adaptive response was substantially attenuated by *Mthl10* knockdown (Fig. 3C).

In addition to immunological and stress-protection responses, recent work (8) has described a vital metabolic role for *GBP* in *Drosophila* larvae. For example, nutrient status sensing by *Drosophila* target of rapamycin (TOR) (19) stimulates the fat body to secrete *GBP*, which releases insulin-like peptides (ILP) from the brain (ref. 8 and Fig. 3D). It is therefore significant that we identified ILP-producing cells within the brain in which both ILP2 and *Mthl10* are coexpressed (Fig. 3E). Moreover, *Mthl10* knockdown decreased ILP2 secretion, as evidenced (14) by the resulting increase in its cellular levels (Fig. 3F). We further discovered that *GBP* overexpression promotes ILP2 secretion (Fig. 3F). In control experiments, we found ILP2 expression in the brain was unaffected by either *GBP* overexpression or by *Mthl10* knockdown (Fig. S8).

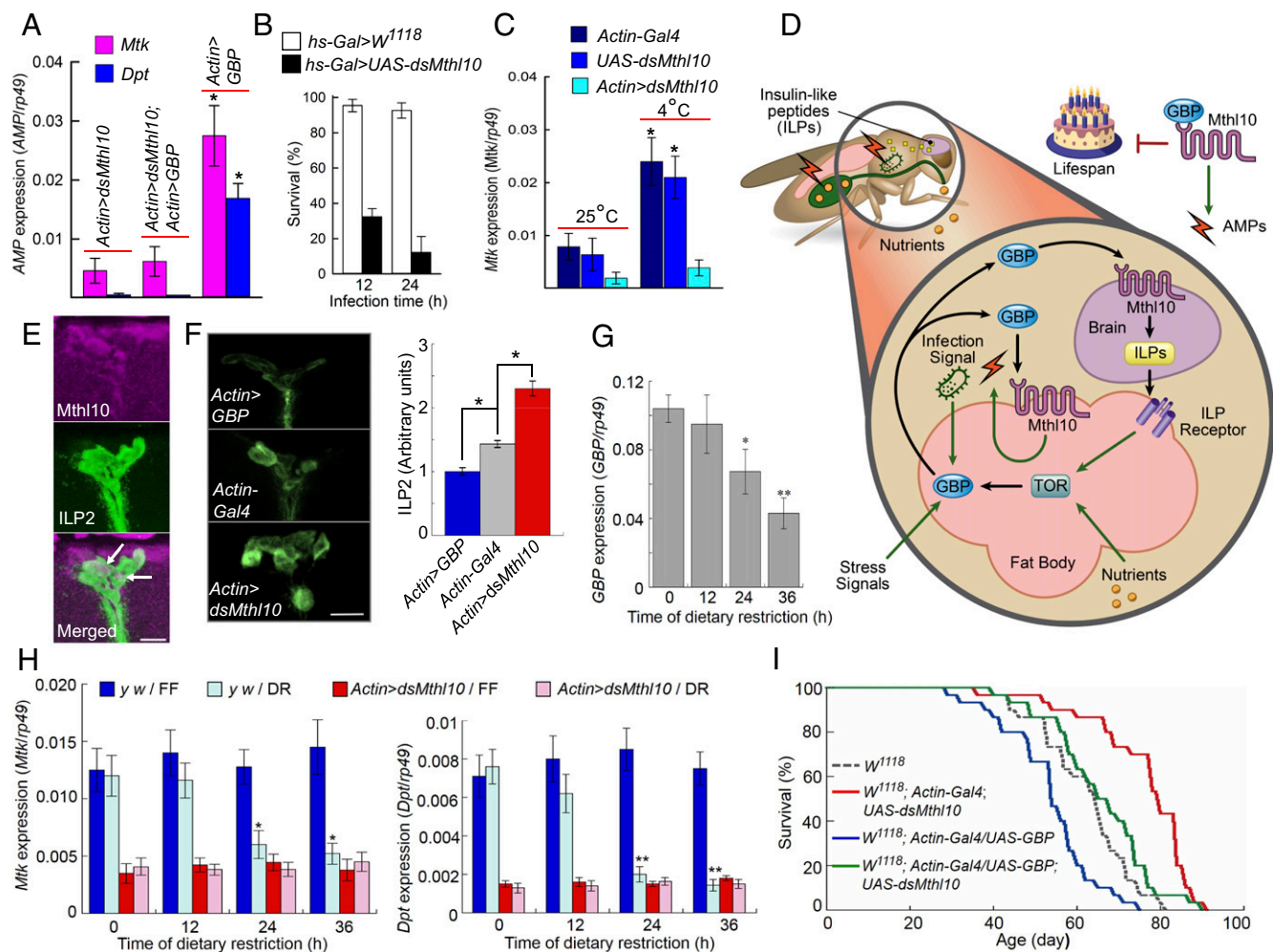


Fig. 3. GBP signaling through *Mthl10* ties lifespan to environmental stress. (A) AMP expression (either *Mtk* or *Dpt*, as indicated) in female *Drosophila* adults (data are means \pm SEM; $n = 8$). (B) Fly survival after bacterial infection; in each experiment, 20 male adults were stabbed with a thin tungsten needle previously dipped into a concentrated culture of *M. luteus*. Values shown are mean \pm SEM ($n = 13$). (C) *Mtk* expression in *Drosophila* larvae maintained at either 25 °C, or 4 °C for 16 h (data are means \pm SEM; $n = 8$). * $P < 0.05$ vs. *Actin > dsMthl10*. (D) Graphic depicting the participation of the GBP/*Mthl10* axis in sensing environmental stress, and the impact upon lifespan. (E) Representative images of *Mthl10* (Top) and ILP2 (Middle) in ILP-producing cells of adult female *Drosophila*. The arrows in the merged image (Bottom) show the overlap of both signals. (Scale bar: 15 μ m.) (F) Reporter assay for ILP2 secretion (8). (Left) Representative images of mean ILP2 immunofluorescence in the ILP-producing cells of *Drosophila* female adult brains. (Scale bar: 15 μ m.) (Right) Relative, mean fluorescence intensities quantified by ImageJ (means \pm SEM; $n = 5$; * $P < 0.05$ vs. *Actin-Gal4*). (G) *GBP* expression levels in dietary restricted female *Drosophila* adult brains (data are means \pm SEM; $n = 6$). * $P < 0.05$, ** $P < 0.01$, vs. zero time. (H) Expression of *Mtk* (Left) and *Dpt* (Right) in dietary restricted (DR) and fully fed (FF) female *y w* and *Mthl10* RNAi strains of *Drosophila* (data are means \pm SEM; $n = 8$). * $P < 0.05$, ** $P < 0.01$, vs. zero time. (I) Effect of *GBP* overexpression and *Mthl10* knockdown on lifespans of *Drosophila* female flies. Lifespan curves of *W¹¹¹⁸*; *Actin-Gal4*; *UAS-dsMthl10* ($P = 1.93 \times 10^{-8}$) and *W¹¹¹⁸*; *Actin-Gal4*; *UAS-GBP* ($P = 3.43 \times 10^{-4}$) were significantly different from control (*W¹¹¹⁸*) (log rank test).

Overall, our data indicate that a close relationship exists between the immunological and metabolic effects of the GBP/Mthl10 axis (Fig. 3D). This is significant because the mounting of an immune response is bioenergetically expensive (20); it takes a considerable energy investment by innate immune cells to synthesize and secrete a battery of cytokines. Coordinating release of ILP2 during stress can mobilize nutrients to satisfy the energetic demands of increased AMP production.

The GBP/Mthl10 Axis Influences Lifespan. An intrinsic property of AMP production is its age-dependent up-regulation (21). It is therefore notable that dietary restriction, which is known to extend lifespan in animals (22–24), is associated with reduced GBP expression in *Drosophila* (ref. 8 and Fig. 3G), which is an anti-inflammatory adaptation. Furthermore, GBP-mediated AMP expression is reduced in dietary-restricted, adult flies (Fig. 3H). It is intriguing that we found this response to dietary restriction to be phenocopied by *Mthl10* knockdown (Fig. 3H). Moreover, the levels of *Mik* and *Dpt* expression in *Mthl10* knockdown flies are equivalent to those observed after 24 h of dietary restriction (Fig. 3H). Conversely, our model (Fig. 3D) predicts that TOR hyperactivation by excess nutrient intake (19) could recruit GBP/Mthl10 to exacerbate metabolic inflammation; this may be one of the reasons that nutrient excess in *Drosophila* can model human metabolic syndrome (19).

These considerations of some of the potential, negative impacts of GBP/Mthl10 signaling led us to study the lifespan of *Mthl10* knockdown flies (Fig. 3I). We found that these flies lived significantly longer than did control *W¹¹¹⁸* lines; in females, *Mthl10* knockdown was associated with a 25% increase in half-survival time compared with control flies. This phenomenon exhibited some sexual dimorphism; the benefit in longevity was less in males (12%; Fig. S9). Interestingly, the well-known impact of dietary restriction upon lifespan is also greatest in female flies (25). Additionally, we found that *GBP* overexpression significantly shortened lifespan compared with the control lines (16% in females; 10% in males; Fig. 3I and Fig. S9). The *GBP*-mediated, shorter-lived phenotype was not observed in a strain with simultaneous knockdown of *Mthl10* (Fig. 3I). Thus, we conclude that *Drosophila* lifespan can be shortened by stress-activated, GBP-Mthl10 signaling pathways (Fig. 3D).

Concluding Comments. The most important development to emerge from this study is the deorphanization of Mthl10, through the placement of this GPCR at the epicenter of a molecular pathway that pits stress responses against lifespan. We show how various immunological and metabolic properties of a single cytokine, GBP, are integrated through its interactions with Mthl10. In particular, we show how the operation of the GBP/Mthl10 axis (Fig. 3D) usefully matches nutrient supply to the degree of a metabolically expensive inflammatory response; this is an important topic in immunology. Our model for GBP/Mthl10 functionality (Fig. 3D) also shows how it has the potential to exacerbate metabolic inflammation; this may be one of the reasons that nutrient excess in *Drosophila* can model human metabolic syndrome (19). Furthermore, we link these homeostatic functions for Mthl10 to its strong influence upon longevity. This provides a molecular foundation for a theory of aging, namely, that a shortened lifespan can be the ultimate price that a young organism pays to successfully combat short-term environmental stresses (26).

We have also considered our findings in relation to previous work (13) that provides a detailed analysis of the expression pattern of *Mthl10* in *Drosophila* embryos and larvae. For example, due to extensive expression of *Mthl10* in imaginal discs, it has been proposed this gene may influence organogenesis (13). It is therefore relevant that cytokines—including the Mthl10 ligand, GBP—are well-known to regulate tissue remodeling and development (27). Additionally, our determination that Mthl10 regulates GBP-mediated innate immune responses (Fig. 2 G and H) seems pertinent to earlier observations (13) that *Mthl10* is expressed in

hematopoietic tissue (which has immunological functions) and also crystal cells, which encapsulate foreign material. Nevertheless, we cannot exclude the possibility that other ligands for Mthl10 remain to be identified, perhaps as a consequence of the expression of alternate *Mthl10* transcripts (13).

The significance of *Mthl10* to longevity and metabolism (Fig. 3 D, H, and I and Figs. S8 and S9) is shared by *Mth* (28, 29). In fact, it was the first gene duplication within the *Mth* superclade that is believed to have given rise to *Mthl10*, which did not then undergo any further expansion in *Drosophila* (12, 13). In contrast, five further rounds of gene duplication apparently occurred before *Mth* emerged (12, 13). Thus, we conclude that the connection between lifespan and metabolic homeostasis that we observed for *Mthl10* is an ancestral trait rather than adaptive specifically to *Mth*.

It is not unusual for gene regulatory networks to be widely conserved, even when certain components might undergo evolutionary turnover (12). Indeed, recent work (30) has shown that although selection pressure has caused GPCR ectodomains and their ligands to codiversify (e.g., Fig. S1), there has nevertheless been considerable conservation of the receptor's intracellular interactions with G proteins; as a result, flies and mammals share many of the same downstream signaling cascades (30). Indeed, GBP exhibits some sequence similarity with the human defensin BD2 (Fig. S1); both are small, cationic cytokines produced by protease action upon larger, precursor proteins (6). Furthermore, human BD2 acts through an uncharacterized GPCR to stimulate PLC/Ca²⁺ signaling to initiate inflammatory responses (31); the current study demonstrates that GBP is also a GPCR ligand that initiates PLC/Ca²⁺ signaling (7, 9). Thus, we propose that there is general applicability to the concepts that emerge from our integration of immunological, metabolic, and lifespan functions for the GBP/Mthl10 axis.

Materials and Methods

Animals and Cells. *Drosophila melanogaster* were normally reared at 25 ± 1 °C on artificial food containing 8.7% (wt/wt) cornmeal, 5.2% (wt/wt) glucose, 3.5% (wt/wt) dried yeast, 0.3% ethyl *p*-hydroxybenzoate, and 1.0% (wt/wt) agar. Under restricted diet condition, flies were reared on special food containing 5.0% (wt/wt) cornmeal, 5.0% (wt/wt) glucose, 1.0% (wt/wt) dried yeast, 0.3% ethyl *p*-hydroxybenzoate, and 1.0% (wt/wt) agar (22). The *UAS-GBP* strain was generated and as described previously (4). The *UAS-dsMthl10* strain was supplied by NIG-FLY (National Institute of Genetics). *Actin-gal4* and *hs-Gal4* strains were derived as described elsewhere (32).

Drosophila S2 cells were supplied by Riken BRC and maintained as previously described (7). *Drosophila* S3 cells were obtained from Karen Adelman, National Institute of Environmental Health Sciences (NIEHS), Research Triangle Park, NC. To prepare S3^{GCaMP3} cells, we subcloned a GCaMP3 transcript (obtained from Karen Adelman) into pAc5.1/V5-His A vectors (Invitrogen) using the EcoRI and XbaI restriction sites (for primers, see Dataset S2); the vector was transfected into S3 cells along with the pCoBlast vector, using a *Drosophila* Expression System (Invitrogen). Both S3 and S3^{GCaMP3} cells were maintained and utilized at 25 °C in Schneider's medium (Gibco) supplemented with 10% heat-inactivated FBS (Invitrogen), 100 units/mL penicillin, and 100 µg/mL streptomycin (Gibco); 25 µg/mL blasticidin (Invitrogen) was added to the culture medium for S3^{GCaMP3} cells.

Primary dsRNA Screen. The dsRNA library was purchased from Harvard/Howard Hughes Medical Institute *Drosophila* RNAi Screening Center (<https://fgr.hms.harvard.edu/>); 0.25 µg/well of dsRNA was used to target each of 1,729 genes that are annotated or computationally predicted to encode transmembrane proteins that it is targeted. The library is provided in duplicate (34 × 384-well plates). The average number of unique dsRNA pairs per gene is two. Each plate is setup with "spare" wells (no added dsRNA), which we utilized for the following controls (Fig. S2): (i) gain of function, using dsRNA against either *Tsr* or *Atx2*; (ii) loss of function controls, using dsRNA against *Itp*; (iii) bland controls, using dsRNA against an irrelevant gene, *LacZ*.

Approximately 10⁴ cells were plated in each well of a dsRNA library plate and incubated in 40 µL of culture medium (see above). After 5 d, GBP-induced fluorescence changes were recorded using a FLIPR^{TETRA} (Molecular Devices) at 25 °C. The excitation wavelength was 488 nm. Fluorescence emission was

selected with a 510- to 575-nm bandpass filter and monitored simultaneously in all wells of a single plate with a cooled charge-coupled device camera.

Total Ca^{2+} released ($[\text{Ca}^{2+}]_T$) was quantified by integrating the area under each “ Ca^{2+} trace.” Z scores were calculated as the mean value of every unique dsRNA pair. A hit was defined by a Z score of less than -1.5 (the mean value for a single dsRNA, assayed in duplicate); $Z \text{ score} = ([\text{Ca}^{2+}]_T \text{ of each dsRNA} - [\text{average } [\text{Ca}^{2+}]_T \text{ of plate}]) / [\text{SD of plate } [\text{Ca}^{2+}]_T]$. The list of Z scores for every gene is available at <https://fgr.hms.harvard.edu/>.

Quantitative Real-Time PCR Analysis. Total RNA was prepared from either S2 cells, adult *Drosophila*, or adult *Drosophila* tissue, as described previously (33). First-strand cDNA was synthesized with oligo(dT)_{12–18} primer using ReverTra Ace RT-PCR kit (Toyobo), according to the manufacturer’s protocol. Real-time quantitative PCR analysis was carried out by using the Light-Cycler 1.3 instrument and software (Roche Applied Science). PCR specificity was confirmed by sequencing of the PCR products and melting curve analysis at each data point.

For assay of gene expression in S3^{GCaMP3} cells, total RNA was isolated from either control- or Mth10-dsRNA treated cells using RNeasy Mini Kit (Qiagen). cDNA was synthesized using SuperScript III First-Strand (Invitrogen) and analyzed by IQ SYBR Green Supermix and IQ5 RT-PCR Detection System (Bio-Rad).

All samples were analyzed in duplicate or triplicate, and assay variation was typically within 10%. Data were normalized according to the expression level of, as indicated, either αTub84D (Tubulin) or *rp49*, determined in duplicate by reference to a serial dilution calibration curve. All primers are listed in Dataset S2.

Statistics. For comparison of tested activities of culture cells and gene expression levels of flies or larvae, Tukey’s honest significant difference tests were carried out. The Shapiro–Wilk test, showed that data sets do not

deviate from the normality. These statistical analyses were performed using JMP 9.0.2 (SAS Institute). Survival ratio comparison was made with the log rank test, using R version 3.2.2 (34). Statistical analysis of Ca^{2+} -signaling dynamics and GBP-TMR binding was performed with a paired t test. Where representative figures are provided, these are one of at least three biological replicates.

Secondary Screening and Orthologous Methodologies. All secondary screening procedures are described in *SI Materials and Methods*.

Mth10 Ectodomain Expression, Purification, and Analysis of Ligand Binding Using Fluorescence Polarization. These procedures are described in *SI Materials and Methods*.

ERK Phosphorylation, Confocal Immunofluorescence, and Cell-Spreading Assays. These procedures are described in *SI Materials and Methods*.

Lifespan Determination. This analysis was performed as described in *SI Materials and Methods*.

Structural Modeling. These procedures are described in *SI Materials and Methods*.

ACKNOWLEDGMENTS. We thank the following for their advice and generosity with their resources: Drs. J. Z. Sexton (from North Carolina Central University), and K. Kim, D. E. Malarkey, G. Travlos, C. D. Bortner, and K. Jeon (from NIEHS). This research was supported by the Intramural Research Program of the NIH, NIEHS, and by Grant-in-Aid for Scientific Research (A) 16H0259 from Japan Society for the Promotion of Science (to Y.H.). The *Drosophila* RNAi Screening Center at Harvard University has received support from NIH Grant NIGMS R01 GM067761.

- Kennedy BK, et al. (2014) Geroscience: Linking aging to chronic disease. *Cell* 159:709–713.
- Irazoqui JE, Urbach JM, Ausubel FM (2010) Evolution of host innate defence: Insights from *Caenorhabditis elegans* and primitive invertebrates. *Nat Rev Immunol* 10:47–58.
- Matsumoto H, Tsuzuki S, Date-Ito A, Ohnishi A, Hayakawa Y (2012) Characteristics common to a cytokine family spanning five orders of insects. *Insect Biochem Mol Biol* 42:446–454.
- Tsuzuki S, et al. (2012) *Drosophila* growth-blocking peptide-like factor mediates acute immune reactions during infectious and non-infectious stress. *Sci Rep* 2:210.
- Hayakawa Y (1990) Juvenile hormone esterase activity repressive factor in the plasma of parasitized insect larvae. *J Biol Chem* 265:10813–10816.
- Shafee TM, Lay FT, Phan TK, Anderson MA, Hulett MD (2017) Convergent evolution of defensin sequence, structure and function. *Cell Mol Life Sci* 74:663–682.
- Tsuzuki S, et al. (2014) Immunophysiological polarization: Switching between humoral and cellular innate immune responses is guided by *Drosophila* cytokine dGBP. *Nat Commun*, 10.1038/ncomms5628.
- Koyama T, Mirth CK (2016) Growth-blocking peptides as nutrition-sensitive signals for insulin secretion and body size regulation. *PLoS Biol* 14:e1002392.
- Zhou Y, et al. (2012) Activation of PLC by an endogenous cytokine (GBP) in *Drosophila* S3 cells and its application as a model for studying inositol phosphate signalling through ITPK1. *Biochem J* 448:273–283.
- Trebak M, Putney JW, Jr (2017) ORAI calcium channels. *Physiology (Bethesda)* 32:332–342.
- Brini M, Carafoli E, Cali T (2017) The plasma membrane calcium pumps: Focus on the role in (neuro)pathology. *Biochem Biophys Res Commun* 483:1116–1124.
- Friedrich M, Jones JW (2017) Gene ages, nomenclatures, and functional diversification of the Methuselah/Methuselah-like GPCR family in *Drosophila* and *Tribolium*. *J Exp Zool B Mol Dev Evol* 326:453–463.
- Patel MV, et al. (2012) Dramatic expansion and developmental expression diversification of the *methuselah* gene family during recent *Drosophila* evolution. *J Exp Zool B Mol Dev Evol* 318:368–387.
- Géminard C, Rulifson EJ, Léopold P (2009) Remote control of insulin secretion by fat cells in *Drosophila*. *Cell Metab* 10:199–207.
- Patel MV, et al. (2016) Gia/Mth15 is an aorta specific GPCR required for *Drosophila* heart tube morphology and normal pericardial cell positioning. *Dev Biol* 414:100–107.
- Sims D, Duchek P, Baum B (2009) PDGF/VEGF signaling controls cell size in *Drosophila*. *Genome Biol* 10:R20.
- West AP, Jr, Llamas LL, Snow PM, Benzer S, Bjorkman PJ (2001) Crystal structure of the ectodomain of Methuselah, a *Drosophila* G protein-coupled receptor associated with extended lifespan. *Proc Natl Acad Sci USA* 98:3744–3749.
- Koppen T, et al. (2011) Proteomics analyses of microvesicles released by *Drosophila* Kc167 and S2 cells. *Proteomics* 11:4397–4410.
- Owusu-Ansah E, Perrimon N (2014) Modeling metabolic homeostasis and nutrient sensing in *Drosophila*: Implications for aging and metabolic diseases. *Dis Model Mech* 7:343–350.
- Lazzaro BP (2015) Adenosine signaling and the energetic costs of induced immunity. *PLoS Biol* 13:e1002136.
- Kounatidis I, et al. (2017) NF- κ B immunity in the brain determines fly lifespan in healthy aging and age-related neurodegeneration. *Cell Rep* 19:836–848.
- Bass TM, et al. (2007) Optimization of dietary restriction protocols in *Drosophila*. *J Gerontol A Biol Sci Med Sci* 62:1071–1081.
- Grandison RC, Piper MD, Partridge L (2009) Amino-acid imbalance explains extension of lifespan by dietary restriction in *Drosophila*. *Nature* 462:1061–1064.
- Tatar M, Post S, Yu K (2014) Nutrient control of *Drosophila* longevity. *Trends Endocrinol Metab* 25:509–517.
- Magwere T, Chapman M, Partridge L (2004) Sex differences in the effect of dietary restriction on life span and mortality rates in female and male *Drosophila melanogaster*. *J Gerontol A Biol Sci Med Sci* 59:3–9.
- Gladyshev VN (2016) Aging: Progressive decline in fitness due to the rising deleterious adjusted by genetic, environmental, and stochastic processes. *Aging Cell* 15:594–602.
- Hayakawa Y (2006) Insect cytokine growth-blocking peptide (GBP) regulates insect development. *Appl Entomol Zool (Jpn)* 41:545–554.
- Lin YJ, Seroude L, Benzer S (1998) Extended life-span and stress resistance in the *Drosophila* mutant *methuselah*. *Science* 282:943–946.
- Delanoue R, et al. (2016) *Drosophila* insulin release is triggered by adipose Stunted ligand to brain Methuselah receptor. *Science* 353:1553–1556.
- Flock T, et al. (2017) Selectivity determinants of GPCR-G-protein binding. *Nature* 545:317–322.
- Niyonsaba F, et al. (2007) Antimicrobial peptides human beta-defensins stimulate epidermal keratinocyte migration, proliferation and production of proinflammatory cytokines and chemokines. *J Invest Dermatol* 127:594–604.
- Takehana A, et al. (2004) Peptidoglycan recognition protein (PGRP)-LE and PGRP-LC act synergistically in *Drosophila* immunity. *EMBO J* 23:4690–4700.
- Ninomiyama Y, Kurakake M, Oda Y, Tsuzuki S, Hayakawa Y (2008) Insect cytokine growth-blocking peptide signaling cascades regulate two separate groups of target genes. *FEBS J* 275:894–902.
- Linford NJ, Ro J, Chung BY, Pletcher SD (2015) Gustatory and metabolic perception of nutrient stress in *Drosophila*. *Proc Natl Acad Sci USA* 112:2587–2592.
- He Y, Jasper H (2014) Studying aging in *Drosophila*. *Methods* 68:129–133.
- Yi NY, et al. (2015) Development of a cell-based fluorescence polarization biosensor using preproinsulin to identify compounds that alter insulin granule dynamics. *Assay Drug Dev Technol* 13:558–569.
- Matsumoto Y, Oda Y, Uryu M, Hayakawa Y (2003) Insect cytokine growth-blocking peptide triggers a termination system of cellular immunity by inducing its binding protein. *J Biol Chem* 278:38579–38585.